# Efficient organic light-emitting diode using semitransparent silver as anode

Huajun Peng, Xiuling Zhu, Jiaxin Sun, Zhiliang Xie, Shuang Xie, Man Wong, and Hoi-Sing Kwok[a)]
*Center for Display Research, Department of Electrical and Electronic Engineering, Hong Kong University of Science and Technology, Clear Water Bay, Hong Kong*

(Received 20 April 2005; accepted 25 August 2005; published online 19 October 2005)

A semitransparent silver layer is investigated as the anode for organic light-emitting devices (OLEDs). By pretreating the silver layer in a $CF_4$ plasma, hole injection into the hole-transport layer is greatly enhanced. A bottom-emitting OLED using the modified, semitransparent silver anode, demonstrates improved current density-voltage characteristics and a 20% higher external quantum efficiency, compared to a conventional OLED using indium tin oxide as an anode. The superior optical characteristics are attributed to a higher outcoupling efficiency in the microcavity structure. © *2005 American Institute of Physics*. [DOI: 10.1063/1.2115076]

Organic light-emitting diodes (OLEDs) have attracted a great deal of attention due to their applications in flat-panel display.[1,2] A typical OLED is composed of a number of organic functional layers sandwiched between two electrodes. In the majority of cases, a thin transparent layer of indium-tin oxide (ITO) on a glass substrate is used as an anode to allow the emission to exit the device. The typical conductivity of ITO is in the range of $1.5-5\times10^3\ \Omega^{-1}\ \mathrm{cm}^{-1}$,[3–5] which corresponds to a sheet resistance of 20–80 Ω/square for a 100 nm thick ITO film. Such high resistance limits the performance of large-area passive-matrix OLED because of the significant voltage drop along the long ITO conducting leads.[2]

Although thicker ITO films exhibit reduced sheet resistance, it also induces more optical modes and higher absorption loss, leading to a lower outcoupling efficiency.[6] Metal shunts can be added along the ITO column lines to improve line conductance. However, the introduction of such metal strips leads to reduced aperture ratio and complicates the fabrication process. Using semitransparent metals as the anode should yield reduced line resistance and less voltage drop. Moreover, it is theoretically proposed that a large enhancement in light extraction efficiency can be achieved by using semitransparent silver anode.[7] However, the reported OLED electrical and optical performance are still poorer than that of a conventional OLED with an ITO anode.[8] Therefore, further investigation is necessary.

Among the metals investigated as anodes for OLEDs are Ni,[9] Au,[10] and Pt.[11] These metals have relative high work functions which give lower barriers for hole injection. However, they are not suitable as the semitransparent anode because absorption loss is quite high. Silver is considered as a potential metal for a semitransparent anode because it has one of the lowest absorptions in the visible light region.[12] Moreover, Ag has the highest electrical conductivity among all these metals. Nevertheless, Ag is generally not considered as a good anode due to its rather low work function (~4.3 eV),[13] leading to a large barrier for hole injection. Recently, Chen *et al.*[14] demonstrated that OLEDs with ultraviolet-ozone pretreated Ag anodes showed electrical characteristics comparable to those of OLEDs with conventional ITO anodes. Hung *et al.*[15] also reported that by pretreating Ag surface in a $CHF_3$ plasma, a significant improvement in hole injection can be achieved. However, both methods employed thick Ag film as the anode for *top-emitting* devices. In this letter, we report the use of a thin (20 nm) Ag layer as the anode in a *bottom-emitting* device. We show that by treating this Ag properly, excellent hole injection can be achieved resulting in a device with performance superior to that of conventional OLEDs with ITO anodes.

To fabricate the device, a patterned 20 nm thick Ag film was first deposited on glass substrate through a shadow mask and then pretreated in a $CF_4$ plasma. The plasma pretreatment was carried out in a home-made plate reactor in a vacuum chamber with a power of 30 W. Our experiment indicated the Ag film could not stand up to the plasma when the power was over 100 W. After anode surface pretreatment, an evaporation chamber with a base pressure of $7\times10^{-7}$ Torr was used for organic film deposition. The organic multilayer structure sequentially consists of alpha-napthylphenylbiphenyl diamine (NPB) (70 nm) as the hole-transport layer, tris-8-hydroxyquinoline aluminum ($Alq_3$) (30 nm) doped with 1 wt % 10-(2-benzothiazolyl)-1,1,7,7-tetramethyl-2,3,6,7-tetrahydro-1H,5H,11H-[1]benzo-pyrano [6,7,8-ij]quinolizin-11-one (C545T) as the emitting layer, and undoped $Alq_3$ (30 nm) as the electron-transport layer. The deposition rates of the organic thin layers were between 0.2 and 0.3 nm/s. The sample was then transferred to another chamber without breaking the vacuum for cathode deposition which was composed of 0.8 nm LiF capped with 120 nm Al.

For comparison, a control device with the same layer structures except the anode was replaced by a 75 nm thick ITO coated on glass substrate was fabricated. The ITO surface was pretreated in an oxygen plasma in the usual manner. Another control device using as-deposited Ag without $CF_4$ pretreatment as the anode was also fabricated. The sheet resistance of 20 nm thick Ag film was measured with four-point probe to be 2 Ω/square. This was more than one order lower than that (25 Ω/square) of the ITO anode in the control device. After fabrication, the devices were characterized in room ambient and temperature without encapsulation. Current-voltage characteristics were measured using an Advantest R6145 dc voltage current source and Fluke 45 dual

[a)]Electronic mail: eekwok@ust.hk

 

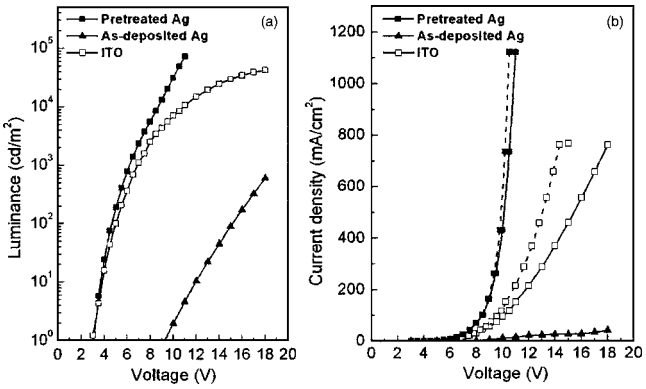


FIG. 1. (a) *L-V* characteristics of the bottom-emitting devices using different anodes. All devices have the configuration of anode/NPB (70 nm)/Alq: 1 wt % C545T (30 nm)/Alq (35 nm)/LiF (0.8 nm)/Al (120 nm). (b) *J-V* characteristics of the devices using different anodes before (solid lines) and after (dashed lines) subtracting the voltage drops along the anode lines.

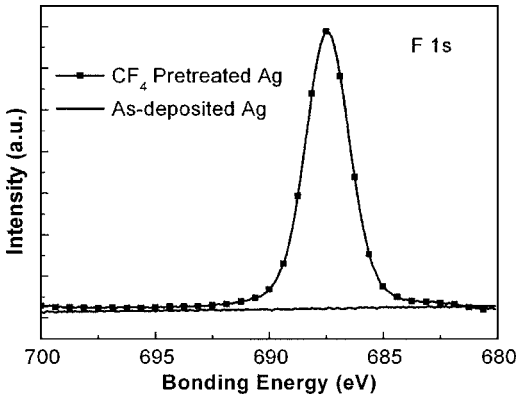


FIG. 2. Core-level F 1*s* XPS spectra of an as-deposited Ag film and a $CF_4$ plasma pretreated Ag film. The thickness was 20 nm for both.

display multimeter. The spectral characterization and electroluminescence intensity were measured using a PR650 SpectraScan spectrophotometer.

Figure 1 compares the current density ($J$)-normal direction luminance ($L$)-voltage ($V$) characteristics of the devices. The data of the conventional ITO anode device is similar to those reported by others.[16] The device with an as-deposited Ag anode shows rather poor performance. On the other hand, the device with modified Ag anode shows performance superior to that of the ITO-based control device, in both *J-V* and *L-V* curves. For instance, the driving voltages at a current density of 100 $mA/cm^2$ for devices with the pretreated Ag and ITO anode are 8.5 and 10 V, respectively. And, the voltages to obtain a luminance of 1000 $cd/m^2$ for the two devices are 6.3 and 6.9 V, respectively. With increased voltage, both the current density and luminance of the pretreated Ag anode device increase faster than those of the ITO anode device, reaching the maximum values of 1120 $mA/cm^2$ and 73 000 $cd/m^2$ at 11 V, respectively. In contrast, the control device with ITO reaches its maximum current density of 760 $mA/cm^2$ and luminance of 42 000 $cd/m^2$ at 18 V. For brevity, the Ag anode device mentioned in the following discussion refers to the device using pretreated Ag as anode.

The superior electrical performance of Ag anode device is attributed to both the lower voltage drop in the anode electrode and enhanced hole injection efficiency. To distinguish between these two effects, we compared the *J-V* curves of Ag anode and ITO anode devices again in Fig. 1(b) by subtracting the voltage drops in the electrodes. The voltage drops were calculated by multiplying the injection current by the electrode resistances which were 5 Ω and 80 Ω for patterned Ag anode and ITO anode, respectively. The larger resistance of ITO results in a bigger voltage drop, especially under high injection current. The intrinsic *J-V* curves indicate that the current density of the Ag anode device is still larger than that of ITO anode device. It infers that $CF_4$ pretreatment can significantly enhance the hole injection ability of Ag anode, making it more effective than the ITO anode.

To investigate the mechanisms responsible for the enhanced hole injection, x-ray photoelectron spectroscopy (XPS) was performed on the treated Ag films. XPS spectra were collected using a Physical Electronics PHI5600 Surface Science Analysis System with Al $K\alpha$ radiation ($h\nu$ = 1486.6 eV). Figure 2 shows the core level of F 1*s* spectra of the as-deposited and the treated Ag film. The spectra of the as-deposited sample are nearly flat indicating no fluorine signals. In contrast, the spectra of the treated sample exhibit a strong peak at approximately 687.5 eV, giving evidence of the existence of rich fluorine bound to C in a $CF_x$ complex. The measured depth profile of the F signal indicates that the $CF_x$ thickness is less than 1 nm. It has been reported that, with an ultrathin insulator layer capping, the anode will enhance the hole injection efficiency.[11,17,18] $CF_x$ polymer is well known to be a good insulating material. In the presence of this $CF_x$ capping layer, the effective barrier against hole injection from the Ag anode into the organic layer can be reduced, leading to an enhanced current density.

We now discuss the effect of the semitransparent silver anode on the device optical performance. At a current density of 100 $mA/cm^2$, the normal direction luminance is 8450 $cd/m^2$ for the Ag anode device, which is about 8% higher than that of 7830 $cd/m^2$ for the ITO anode device. In a conventional bottom emitting ITO-OLED, the emission profiles are usually Lambertian. However, it is not true for the Ag anode device because of the high reflectivity of the Ag anode. Figure 3 shows the measured reflection and transmission spectrum of the Ag anode and the ITO anode with multilayer organic films on top. The reflectivity of the Ag anode is over 55%, much higher than that of ITO anode, in the range between 500 nm and 700 nm. The bottom emitting

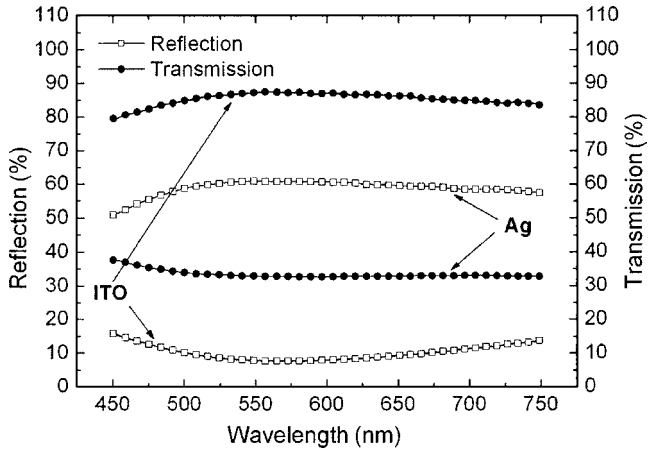


FIG. 3. Reflection and transmission spectrum of the 20 nm Ag anode and the 75 nm ITO anode with organic layers coated on top. The multilayer structure consists of substrate/anode/NPB (70 nm)/Alq: 1 wt % C545T (30 nm)/Alq (35 nm).

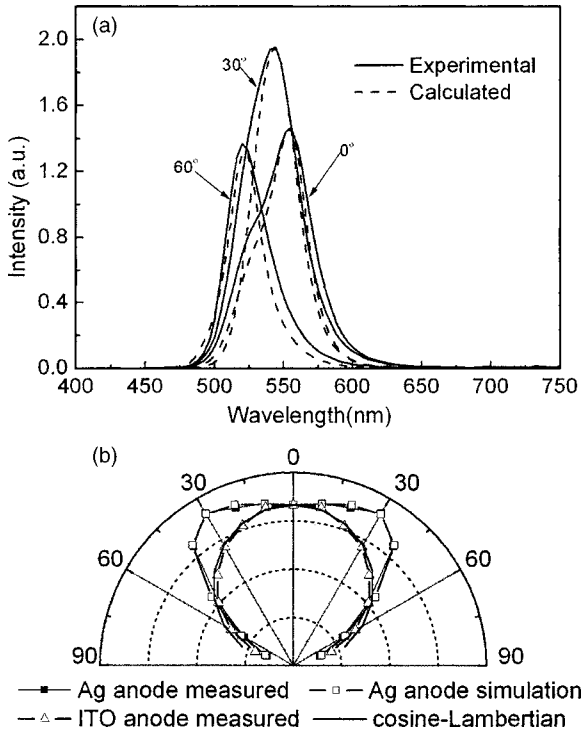


FIG. 4. (a) Comparison of the simulated (dashed lines) and experimentally measured (solid lines) spectral characteristics at different viewing angles for the Ag anode device The simulated spectra are all scaled by the same constant factor for an optimum fit to the experimental data. (b) Angular distribution of photon radiation intensity for the Ag anode device and the ITO anode device. All intensities are normalized relative to that of the normal direction.

device with reflecting anodes and cathodes is expected to exhibit strong microcavity effects on both the spectral and spatial distributions of the emission.

Figure 4(a) shows the electroluminescence (EL) spectra measured under a current of 20 $mA/cm^2$ at viewing angles of 0°, 30°, and 60° off the normal direction for the Ag anode. A blueshift in the spectral peak with increasing angular displacement from the normal is observed, from 552 nm at 0° to 520 nm at 60°. The angular dependent luminance intensities of both OLEDs were measured and normalized intensities computed using the respective normal direction intensities as the bases. The corresponding angular distributions are compared in Fig. 4(b). It is clear that while the angular dependence of the ITO anode device is well fitted by a Lambertian distribution, the same is not true for the Ag anode device. In fact, the highest luminance was measured at ~30° from the normal. The strong microcavity effects in the Ag anode device can also be quantified using a classical model which calculates the spontaneous radiation of dipoles in thin film microcavities.[19,20] The simulated EL spectra and spatial emission pattern are given in Figs. 4(a) and 4(b), respectively. It is found the calculated results agree very well with the experimental results.

For the non-Lambertian radiation, the external quantum efficiency ($\eta_E$) of the OLED is evaluated by integrating the photon flux using the formula $\eta_E = 2\pi / J \Sigma I(\theta) \sin(\theta) \Delta\theta$, where $I(\theta)$ is the measured photon radiation intensity at angle $\theta$. It is found that $\eta_E$ of the Ag-anode device is about 20% higher than that of the ITO anode control device in the forward 140° cone. The enhancement of emission into air is due to the enhanced spontaneous emission and the modified emission distribution as the consequences of the strong micro-cavity effect in the Ag anode device.

It has been shown that the spontaneous emission rate and hence the total emission of the oscillating dipoles can be enhanced in the metal mirror microcavity structure.[7,21] Assuming a one-dimensional microcavity, the spontaneous emission rate of the dipole is calculated to be 10% larger in the Ag anode device than in ITO anode device. At the same time, due to the high reflectivity of the electrodes, multiple-beam interference becomes strong in the cavity device, altering the internal angular power distribution. With an appropriate design of the cavity structure, the preferential propagation direction of the photons can thus be forced from total internal reflection regime toward the extraction cone, benefiting the outcoupling efficiency.[22] In the present Ag anode device, the emission is enhanced at the emitting cone of ±50°, but suppressed at the larger viewing angles. The total emission enhancement due to the redistribution effect is ~10%.

In summary, we show that a $CF_4$ plasmas treated semitransparent Ag film can be used as an effective anode for bottom emitting OLEDs. The $CF_4$ plasma pretreatment can greatly enhance the hole injection ability of the Ag film. In comparison with the conventional bottom-emitting device using the ITO anode, the Ag anode devices show superior current voltage characteristics and emit 20% more photons in the forward 140° cone. The superior optical performance of the Ag anode device is attributed to the employment of the semitransparent Ag anode to form a microcavity structure.

This research was supported by the Hong Kong Government Innovations and Technology Fund.

[1] C. W. Tang and S. A. VanSlyke, Appl. Phys. Lett. **51**, 913 (1987).
[2] G. Gu and S. R. Forrest, IEEE J. Sel. Top. Quantum Electron. **4**, 83 (1998).
[3] M. Higuchi, S. Uekusa, R. Nakano, and K. Yokogawa, Jpn. J. Appl. Phys., Part 1 **33**, 302 (1994).
[4] K. Sreenivas, T. Sundarsena Rao, A. Mansnigh, and S. Chandra, J. Appl. Phys. **57**, 384 (1985).
[5] J. Szczyrbowski, A. Dietrich, and H. Hoffmann, Phys. Status Solidi A **78**, 243 (1983).
[6] M.-H. Lu and J. C. Sturm, J. Appl. Phys. **92**, 595 (2002).
[7] K. Neyts, P. D. Visschere, D. K. Fork, and G. B. Anderson, J. Opt. Soc. Am. B **17**, 114 (2000).
[8] K. Tamano, D. C. Cho, T. Mori, T. Mizutani, and M. Sugiyama, Thin Solid Films **438**, 182 (2003).
[9] M. H. Lu, M. S. Weaver, T. X. Zhou, M. Rothman, R. C. Kwong, M. Hack, and J. J. Brown, Appl. Phys. Lett. **81**, 3921 (2002).
[10] R. A. Hatton, M. R. Willis, M. A. Chesters, F. J. Rutten, and D. Briggs, J. Mater. Chem. **13**, 38 (2003).
[11] C. F. Qiu, H. J. Peng, H. Y. Chen, Z. L. Xie, M. Wong, and H. S. Kwok, IEEE Trans. Electron Devices **51**, 1207 (2004).
[12] P. B. Johson and R. W. Christy, Phys. Rev. B **6**, 4370 (1972).
[13] H. B. Michaelson, IBM J. Res. Dev. **22**, 72 (1978).
[14] C. W. Chen, P. Y. Hsieh, H. H. Chiang, C. L. Lin, H. M. Wu, and C. C. Wu, Appl. Phys. Lett. **83**, 5127 (2003).
[15] Z. Xie, L. S. Hung, and F. Zhu, Chem. Phys. Lett. **381**, 691 (2003).
[16] H. Kanno, Y. Hamada, and H. Takahashi, IEEE J. Sel. Top. Quantum Electron. **10**, 30 (2004).
[17] I. M. Chan, T. Y. Hsu, and F. C. Hong, Appl. Phys. Lett. **81**, 1899 (2002).
[18] C. Qiu, Z. Xie, H. Chen, M. Wong, and H. S. Kwok, J. Appl. Phys. **93**, 3253 (2003).
[19] W. Lukosz and R. E. Kunz, J. Opt. Soc. Am. **67**, 1607 (1977).
[20] H. J. Peng, Y. L. Ho, X. J. Yu, and H. S. Kwok, J. Appl. Phys. **96**, 1649 (2004).
[21] H. Becker, S. E. Burns, and R. H. Friend, Phys. Rev. B **56**, 1893 (1997).
[22] D. Delbeke, R. Bockstaele, P. Bienstman, R. Baets, and H. Benisty, IEEE J. Sel. Top. Quantum Electron. **8**, 189 (2002).